








Optimising aboveground biomass estimation in rubber plantations using vegetation indices derived from Landsat 8 OLI-TIRS imagery

Iqbal Putut Ash Shidiq^{*1} , Mohd. Hasmadi Ismail² , Mohammad Firuz Bin Ramli² ,
Norizah Kamarudin² , Pakhriazad Hassan Zaki² ,
Mohamad Azani Alias² , Rokhmatuloh Rokhmatuloh¹ 

¹) Universitas Indonesia, Faculty Mathematics and Natural Sciences, Department of Geography,
Jl. Lingkar, Pondok Cina, Kecamatan Beji, 16424, Depok, Indonesia

²) Universiti Putra Malaysia, Faculty of Forestry and Environment, 43400 UPM, Serdang, Selangor, Malaysia

* Corresponding author

RECEIVED 14.02.2025

ACCEPTED 03.09.2025

AVAILABLE ONLINE 12.12.2025

Abstract: Rubber plantations in Southeast Asia have been identified as one of major contributors to deforestation and habitat degradation in the region, primarily when they replace natural forests. However, despite these environmental concerns, well-managed rubber plantations can support sustainability efforts, including climate change mitigation, sustainable land management practices, renewable energy development, environmental conservation, and economic viability. Among the key components, aboveground biomass (AGB) is particularly important in regulating potential carbon emissions from rubber plantations. Therefore, this study aimed to develop an optimal statistical model for estimating the AGB of rubber plantations by utilising several vegetation indices (VIs) derived from Landsat 8 OLI-TIRS satellite imagery. To achieve this, both linear and non-linear regression tests were conducted. Furthermore, vegetation and landscape properties were included as inputs to differentiate the variance of *Vis* influence on AGB prediction. The developed model serves as a fundamental algorithm for generating a map that predicts the AGB within the study area. Additionally, the distribution of biomass on the surface was estimated based on models A and B, which were further divided into three age groups and two landscape categories. The statistical analysis showed a strong similarity between the estimated and observed AGB, with a difference of less than 1%. The results indicated that the mathematical model for these variables aligns more closely with non-linear regression rather than its linear counterpart. This was evidenced by the R^2 value, which increased fivefold for non-linear regression.

Keywords: aboveground biomass, *Hevea brasiliensis*, regression modelling, remote sensing, vegetation indices

INTRODUCTION

Forest ecosystems, including rubber tree plantations, are vital components of terrestrial ecosystems that facilitate the exchange of CO₂ with the atmosphere. Rubber trees (*Hevea brasiliensis*) are extensively cultivated in tropical regions for latex production (Goh, Lee and Kok, 2013). While rubber plantations are primarily managed for economic purposes, they still contribute to carbon sequestration. The aboveground biomass of rubber trees stores a significant amount of carbon (Shidiq and Ismail, 2016), and

appropriate management practices can enhance their potential for carbon sequestration (Jat *et al.*, 2022). In the modelling of the carbon balance of terrestrial ecosystems, biomass is often required as a model input due to its impact on autotrophic respiration and carbon transfer to the soil (Zheng *et al.*, 2007). Biomass plays a significant role in climate change studies by providing valuable insights into the net CO₂ equivalent from the terrestrial ecosystem (Houghton *et al.* (eds.), 1995).

The rapid expansion of rubber plantations in Southeast Asia has become a major driver of deforestation and various

forms of habitat degradation (Chapman, 1991; Ziegler, Fox and Xu, 2009; Li and Fox, 2012; Fan *et al.*, 2015). These negative processes can be attributed to the increasing demand for processed forest products, such as wood, latex, palm, and mangrove, which are commonly used for industrial purposes. Despite the degraded state of these plantations, they still actively contribute to the forest supply area, particularly in maintaining green coverage beyond the region. Extensive research has explored the environmental and socioeconomic impacts of rubber expansion at various scales, aiming to gain a comprehensive understanding of the plantation's role in balancing the carbon cycle within the terrestrial ecosystem (Fan *et al.*, 2015; Anurogo, Lubis and Mufida, 2018).

Over the past few decades, there has been a growing interest in estimating aboveground biomass (AGB) using remotely sensed data, including field measurements and model estimations (Lu, 2005; Zheng *et al.*, 2007). For instance, Hui (1999) and Sone *et al.* (2014) proposed models for estimating biomass based on parameters such as diameter at breast height (DBH), tree height, crown size, crown length, and crown volume. However, acquiring these measurements is time-consuming and labour-intensive, making it impractical for large-scale applications (Zheng *et al.*, 2007). Other studies have employed traditional methods, such as the dry-weighted algorithm, to calculate biomass (Fang *et al.*, 1998; HariPriya, 2000). Therefore, AGB can be directly estimated using remotely sensed data with different approaches, including multiple regression analysis, *k*-nearest neighbour, and neural network (Roy and Ravan, 1996; Steininger, 2000; Nelson *et al.*, 2001; Foody, Boyd and Cutler, 2003; Zheng *et al.*, 2004). Additionally, estimation can be attempted using biophysical parameters derived from vegetation indices (VIs) and remotely sensed data, such as canopy covers, crown diameter, leaf area index, and chlorophyll content. Mathematical models developed in previous studies have been employed for these calculations (Wu and Starhler, 1994; Phua and Saito, 2003; Popescu, Wynne and Nelson, 2003; Zheng *et al.*, 2007).

The spectral reflectance of VIs has been widely utilised for AGB estimation. Numerous VIs have been developed and applied in studies focusing on biophysical parameters (Anderson and Hanson, 1992; Anderson, Hanson and Haas, 1993; Eastwood *et al.*, 1997; Lu *et al.*, 2004; Mutanga and Skidmore, 2004). They are recommended to mitigate variability caused by canopy cover, soil background, sun view angles, and atmospheric conditions during biophysical property measurements (Elvidge and Chen, 1995; Lu, 2005). Several evaluation-based VIs have been widely used in AGB estimation by applying various mathematical adjustments and alterations. Some of the most commonly used VIs are leaf area index – LAI (Zhang *et al.*, 2014; Dong *et al.*, 2016; Wang *et al.*, 2019), normalized difference vegetation index – NDVI (Zhu and Liu, 2015), simple ratio index – SR (Zheng *et al.*, 2007), and the soil-adjusted vegetation index – SAVI – family (Yan, Wu and Wang, 2013). Prior to these studies, the compatibility of VIs has been developed to enhance their applicability across diverse sites and forest conditions.

While many studies utilise VIs for aboveground biomass (AGB) estimation, they often rely on simplified approaches and limited field data. This research distinguishes itself by integrating a comprehensive dataset of ground-measured rubber tree biophysical properties, including stand age and landscape characteristics, with advanced VIs derived from Landsat 8 OLI-

TIRS satellite imagery, enabling the development of a more robust and optimised AGB estimation model. The primary objective of this study is to formulate this enhanced statistical model for estimating AGB, utilising several VIs from Landsat 8 OLI-TIRS satellite imagery. The analysis primarily involves stand age parameters and landscape properties as variable inputs to enhance the robustness of the results. The initial estimation of AGB, obtained from an allometric equation (Heriansyah *et al.*, 2025), serves as the dependent variable, with the VIs acting as predictors. Furthermore, the developed model is used as a basic algorithm to generate a predicted AGB map of the study area. This map provides an overview of the distribution based on the step-by-step fragmentation of remote sensing and biomass modelling. The entire modelling process also defines factors that are less and more significant, thereby being sensitive to the dynamics of AGB estimation.

MATERIALS AND METHODS

STUDY AREA

The study area is located in Felda Lubuk Merbau, which falls under the administration of the Federal Land Development Authority (FELDA), a national government agency. The absolute coordinates of the study area range from 5°58'54" to 6°2'6"N and from 100°40'48" to 100°44'24"E (Fig. 1). It is situated in the northwestern part of Peninsular Malaysia, specifically within the district of Sik in the state of Kedah. The area covers 2,906 ha, with approximately 50% of the land planted with rubber trees. The topography varies, encompassing both flat plains and hilly terrain, with elevations ranging from 40 to 500 m a.m.s.l. The primary cultivated commodity in the area is rubber trees, which are between 5 and 20 years old (Shidiq and Ismail, 2016).

SATELLITE DATA

For this study, the primary data source utilised was Landsat 8 OLI-TIRS imagery, specifically captured over path 128, row 056. This satellite carries two advanced science instruments – the Operational Land Imager (OLI) and the Thermal Infrared Sensor (TIRS). These instruments together provide comprehensive coverage of the Earth's landmass with multiple spectral bands, offering a spatial resolution of 30 m for visible, near-infrared (NIR), and shortwave infrared (SWIR) bands, 100 m for the thermal band, and 15 m for the panchromatic band. To ensure accurate geolocation and precise spatial referencing for subsequent analysis and measurements, the obtained Landsat 8 OLI-TIRS imagery was geo-rectified to the Universal Transverse Mercator (UTM) projection, specifically zone 47N, which corresponds to the study area in Peninsular Malaysia. Geo-rectification is a crucial process that corrects geometric distortions in satellite imagery to align it with a standardised coordinate system, enabling precise spatial analysis and measurements.

Landsat 8 was chosen as the primary data source for deriving VIs due to its extensive coverage and free global data availability, which is highly beneficial for large-scale environmental monitoring and offers a suitable spatial resolution for mapping biomass at the plantation level. However, a known limitation inherent to optical remote sensing, including Landsat 8,

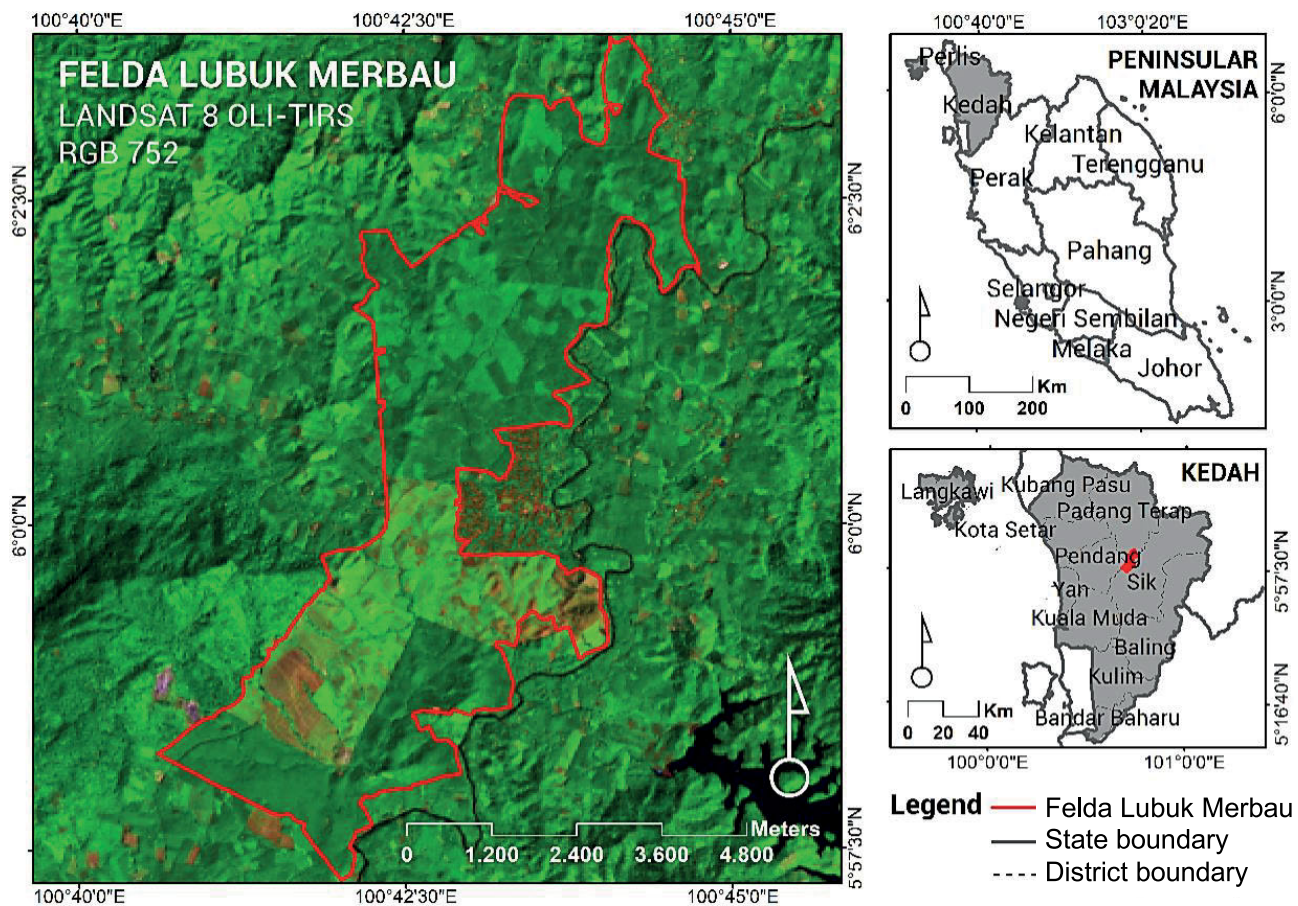


Fig. 1. Study area of Felda Lubuk Merbau, Kedah, Malaysia; source: own elaboration

is its susceptibility to cloud cover, which can significantly hinder data acquisition in frequently cloudy tropical regions. Furthermore, in very dense vegetation areas, the signal may reach saturation, potentially affecting the accuracy of biomass estimation at higher ranges. Following the data acquisition and georectification, initial pre-processing steps, such as atmospheric and radiometric corrections, were performed on the imagery prior to further analysis and the derivation of VIs.

The selection of 2015 as the specific research period was primarily driven by two critical factors, ensuring the scientific rigour and relevance of our AGB estimation model. Firstly, this year provided optimal availability of high-quality, relatively cloud-free Landsat 8 OLI-TIRS imagery for our study area in Peninsular Malaysia. Acquiring suitable optical satellite imagery in tropical regions frequently presents challenges due to persistent cloud cover, and the data from 2015 allowed us to minimise atmospheric interference, which was paramount for accurate vegetation index derivation and subsequent AGB modelling. Secondly, the 2015 period also coincided directly with the collection of comprehensive ground-truth data on rubber tree biophysical properties and stand age, which was essential for calibrating and validating our allometric equations and statistical models. Synchronising the satellite imagery acquisition with the ground measurement period is vital for minimising temporal discrepancies, thereby significantly enhancing the accuracy and reliability of our AGB estimations. While previous research on AGB estimation in rubber plantations has explored earlier satellite missions such as Landsat 5 TM and Landsat 7 ETM+ for different periods, our study uniquely leverages the enhanced spectral

capabilities and improved calibration of Landsat 8 OLI-TIRS. Our specific focus on optimising statistical models by integrating detailed ground-measured tree properties with this more advanced Landsat 8 data for rubber plantations in this particular year represents a distinct contribution, aiming for improved accuracy and a nuanced understanding that complements prior investigations using older datasets.

FIELD DATA COLLECTION AND PLOT-LEVEL BIOMASS

The ground data collection was conducted from January to February 2015. A systematic approach was employed, where a rectangular plot measuring 30×30 m was created to collect rubber tree samples. In total, 196 trees were initially collected as samples. However, one was excluded due to inadequate information, making a total of 195. The plots were evenly distributed across the study area, considering four different age groups, such as 5, 10, 15, and 20. Two primary dimensions collected from the plot were the diameter at breast height (DBH) and tree height. The average DBH was approximately 70.78 cm, with the lowest and highest values being 39.38 and 110.40 m, respectively. In terms of tree height, the range varied from 6.27 to 8.62 m, with a relatively consistent distribution across the observed values, as presented in Table 1.

Before the statistical analysis, some changes were made to the data structure of the sample plots resulting from remote sensing. Both the original Landsat 8 OLI-TIRS pixel and the sample plot sizes were 30×30 m. However, since the Landsat 8 panchromatic band generates a smaller pixel size, the data

Table 1. Statistics of tree's physical properties of rubber plantation in Felda Lubuk Merbau

Grouping	Number of samples	Diameter at breast height (DBH, cm)			Height (m)		
		mean	min.	max.	mean	min.	max.
All age groups	66	70.78	39.38	110.40	7.13	6.27	8.62
Age 5–10 years old	30	64.09	39.38	102.40	6.93	6.27	7.52
Age 15–20 years old	36	76.36	40.60	110.40	7.29	6.77	8.62
Valley	30	73.06	39.38	102.40	7.09	6.35	7.63
Hill	36	68.88	40.60	110.40	7.16	6.27	8.62

Source: own elaboration.

structure was modified. The number of biomass plots used in statistical analysis was reduced to 66 plots with pixel sizes 15×15 m. The number of sample plots also corresponds to the total VIs generated from the Landsat 8 data, which were subsequently applied in regression analysis. Furthermore, the sample plots were categorised based on tree age and landscape properties (topography). In terms of tree age, the plots were divided into two groups of 5–10 and 10–20 years.

INITIAL ABOVEGROUND BIOMASS CALCULATION

In this study, the initial calculation for AGB was derived from the biomass estimation results discussed in the previous chapter. This value was used as the dependent variable in the regression analysis and is referred to as the observed AGB in subsequent analyses. Two (2) different allometric equations were applied to calculate AGB based on the DBH, which serves as the main and single input of the formula. These allometric equations are species-specific to rubber plantations in tropical regions. Furthermore, the presentation of the observed value has been shifted following the number of sample plots used in this specific chapter. Equations (1) and (2) represent the allometric equations developed by Dey *et al.* (1996) and Shorrocks, Templeton and Iyer (1965), respectively.

$$AGB = 0.0202D^{2.249} \quad (1)$$

$$AGB = 0.002604D^{2.7826} \quad (2)$$

where: D = trunk diameter or diameter at breast height (DBH), cm.

IMAGE PRE-PROCESSING

Landsat 8 OLI-TIRS image of Felda Lubuk Merbau (path 128, row 056) level-1 precision terrain-corrected product (L1TP) was downloaded from the Earth Explorer (EE) webpage (<https://earthexplorer.usgs.gov>). It was geometrically corrected by the system, creating sophisticated imagery that followed the compatible map projection and orientation (USGS, 2019). The image pre-processing steps include radiometric calibration, atmospheric correction, image subset, and pan-sharpening.

The radiometric calibration process adhered to the guidelines outlined in the Landsat 8 data users handbook provided by the USGS (2019). The original digital number (DN) was

converted to a spectral radiance value at a sensor level. Furthermore, the atmospheric correction follows the Fast Line-of-Sight Atmospheric Analysis of Spectral Hypercubes (FLAASH) module executed in ENVI 5.0 software (L3Harris Geospatial, USA, Commercial license). This module was chosen for its ability to handle multi-spectral sensors and effectively eliminate atmospheric noise while maintaining the reflective spectral characteristics of surface features (Yuan and Niu, 2008; Guo and Zeng, 2012).

Another step in the pre-processing phase was the implementation of image pan-sharpening. This procedure involved merging a high-resolution panchromatic image with low-resolution multi-spectral images to generate a high-resolution multi-spectral image (Sekreka, Kedzierski and Wierzbicki, 2019). To accomplish this, the Gram–Schmidt method was employed for pan-sharpening, following the recommendation by (Laben and Brower, 2000).

IMAGE PROCESSING

In the image processing step of this study, VIs were extracted to capture relevant information about the rubber plantations. The selected VIs were chosen to represent distinct groups of vegetation characteristics and provide insights into canopy cover, green leaf chlorophyll content, and sensitivity to the biophysical parameters of the vegetation. The leaf area index (LAI), normalised difference vegetation index (NDVI), green normalised difference vegetation index (GNDVI), and modified simple ratio (MSR) were primarily related to canopy cover, green leaf chlorophyll, and sensitivity to vegetation's biophysical parameter. However, soil adjusted vegetation index (SAVI) and optimised soil adjusted vegetation index (OSAVI) were more focused on minimising the influence of the soil background on the surface (Bagheri *et al.*, 2012). The VIs applied in this study are presented in Table 2. The selection of these VIs allowed for a comprehensive characterisation of the rubber plantations and their biophysical properties, enabling accurate estimation of AGB and the subsequent analysis conducted in the study.

STATISTICAL TEST AND BIOMASS MODELLING

Statistical analysis was essential for determining the best model that captured the influence of several predictors on the estimated AGB value. Furthermore, the result was applied to create a predicted map across the area of Felda Lubuk Merbau. To establish the best relationship model between AGB and VIs,

Table 2. Definition and source of VIs used in this study

Vegetation index	Formula	Reference
Enhanced vegetation index (EVI)	$2.5(\rho N - \rho R)/(\rho N + 6\rho R - 7.5\rho B + 1)$	Huete <i>et al.</i> (2002)
Leaf area index (LAI)	$3.618EVI - 0.118$	Boegh <i>et al.</i> (2002)
Normalised difference vegetation index (NDVI)	$\rho N - \rho R/\rho N + \rho R$	Rouse <i>et al.</i> (1974)
Green normalised difference vegetation index (GNDVI)	$\rho N - \rho G/\rho N + \rho G$	Gitelson, Kaufman and Merzlyak (1996)
Soil adjusted vegetation index (SAVI)	$\rho N - \rho R(1 + L)/(\rho N + \rho R + L);$ $L = 0.5$	Huete (1988)
Optimised soil adjusted vegetation index (OSAVI)	$\rho N - \rho R(\rho N + \rho R + 0.16)$	Rondeux, Steven and Baret (1996)
Modified simple ratio (MSR)	$\rho N\rho R - 1\rho N\rho R + 1$	Chen (1996)

Explanations: ρ = spectral reflectance (or reflectance), N = near infrared (NIR), G = green, R = red, L = soil noise factor.

Source: own elaboration.

this study explored both linear and non-linear regression tests. The non-linear model demonstrated a better fit compared to the linear test, which aligned with previous results indicating a non-linear relationship between biomass and tree physical properties such as *DBH* and height (Sone *et al.*, 2014). Another study conducted by Qi *et al.* (1994) also supported this notion by highlighting the non-linear relationship between the green band, particularly *NDVI*, with canopy structure and chemical content. However, to attain a comprehensive comparison among all the models, this study examined both linear and non-linear regressions, with the selection of the preferred model based on the highest R^2 value, indicating a better correlation between the two variables.

The initial test conducted was the linear model, which technically applied stepwise regression analysis. It regressed all predictor variables, such as the six VIs, namely *LAI*, *NDVI*, *GNDVI*, *MSR*, *SAVI*, and *OSAVI* toward the initial *AGB* values. The dataset passed through various transformations including logarithmic, square root, and inverse, for both dependent and predictor variables. However, the test results indicated very low R^2 (<0.35) for all models, necessitating further analysis tests to interpret the data and establish relationships.

In the non-linear test, no data transformation was applied unlike in the linear model. Each running test in the non-linear analysis focuses on a single independent variable instead of computing all VIs simultaneously. This approach allows for a more transparent relationship between *AGB* and each VI, elucidating distinct correlations between the two variables. Several different non-linear functions were considered, and the best model was determined based on the highest R^2 and a confidence level exceeding 90%. Furthermore, this study involved the vegetation and landscape properties as inputs to

distinguish the variance of *Vis*' influence on *AGB* prediction. The stand age parameter and landscape properties are applied as categories to segment the pixels. Each category runs similar steps of analysis, resulting in different models with varying R^2 values and significant levels. Finally, the tests were executed using the statistical program STATA MP 13 (StataCorp LLC, USA, Commercial license).

RESULTS AND DISCUSSION

CHARACTERISTICS OF MEASURED ABOVEGROUND BIOMASS (AGB)

Three different classifications were introduced to describe *AGB* values, each corresponding to a specific calculation method. They are crucial for highlighting the role and purpose of *AGB* values in each discussion, as well as establishing their specific relationship with other predictors. A brief explanation of these classifications is provided in Table 3.

BIOMASS MODEL DEVELOPMENT

The development of biomass models involved several types of statistical tests. In this study, both linear and non-linear tests were employed to determine the most suitable model of biomass and VIs, considering adjustment in sample grouping based on age and landscape properties. The observed *AGB* was utilised as the dependent variable. In the non-linear tests, the models were divided into two main categories based on the basic allometric equations used as calculation functions. Models A and B were developed from observed *AGB* calculated from the equation

Table 3. The classifications of aboveground biomass (*AGB*) value

Classification of <i>AGB</i> value	Basic calculation
Observed <i>AGB</i>	Value of <i>AGB</i> was calculated from two initial allometric equations by Dey <i>et al.</i> (1996) and Shorrocks, Templeton and Iyer (1965).
Estimated <i>AGB</i>	<i>AGB</i> value resulted from statistical tests against the number of samples divided into five different groups.
Predicted <i>AGB</i>	<i>AGB</i> value resulted from prediction models developed through the statistical tests and executed in the entire study area.

Source: own elaboration.

proposed by Dey *et al.* (1996) and Shorrocks, Templeton and Iyer (1965), respectively. Subsequently, further analysis led to the development of models A1–A5 and B1–B5, corresponding to the respective sample groupings explained earlier.

Non-linear model of AGB and vegetation indices

In this study, various non-linear functions were applied to two different observed AGB equations and six VIs. The selection of the most suitable model involved considering a confidence level of over 90% or a p -value < 0.1 to ensure the expected relationship was adequately explained. The R^2 value of the all-age groups category significantly increased to 0.66 (model A1) and 0.61 (model A2) when compared to the linear model (Tab. 4). In this case, VIs explain 60–70% of the variance in the relationship with AGB. Similar results were observed in other categories, such as the 15–20-year group (models A3 and B3), which gained an R^2 value of 0.71. These values sufficiently explain the relationship between VIs and estimated AGB, which varies significantly in direction. Among the five categories, only the 5–10-years group (models A2 and B2) showed a positive direction, indicating that a greater index value corresponds to a higher estimated AGB. Meanwhile, other categories exhibit a negative direction, implying that a higher index value results in a less dependent variable. To gain a clearer understanding of the relationship between the variables, Figure 2 provides visual representations.

The most significant among the VIs is SAVI which is applied in six models, namely A1, A4, A5, B1, B4, and B5. OSAVI appears in A3 and B3, while GNDVI is present in A2 and B2. The distinct tendency of A2 and B2 models is that they have a positive relationship with the VI, despite employing different types of non-linear formulas. The exponential formula proves to be a fit model with a slightly high R^2 value for the 5–10-years-old group (models A2 and B2). Meanwhile, other groups yield a non-linear formula as the best model.

The overall R^2 value of model A is higher than that of model B, with an average gap of about 4%. This indicates that model A is more compatible with explaining the relationship between the two variables. The observation is further explained by the value of RSME, which is lower for model A than model B. However, to conduct a more comprehensive analysis and comparison of the predicted AGB map, this study included all models from both equations. It is also expected that the equations can effectively describe the dynamics of VIs and AGB relationship of the plantation in Felda Lubuk Merbau.

Relationship of AGB and vegetation indices

The results of this study indicated that VIs can be good predictors for estimating AGB. Previous studies have highlighted the challenges associated with biomass estimation from optical data, specifically in humid tropical forests characterised by a complex, multi-layered closed canopy structure combined with a high level of biomass (Steininger, 2000; Foody, Boyd and Cutler, 2004; Nelson, Short and Valenti, 2004; Thenkabail *et al.*, 2004; Lu, 2005; Goh *et al.*, 2013). However, few studies have shown positive results in estimating tropical forest biomass despite the inclusion of other factors such as forest stand structure, climate, and terrain conditions. This is in line with this study conducted by Nelson, Short and Valenti (2004), Lu (2005), Sarker and Nichol (2011). It should be noted that not all VIs were directly correlated with biomass (Foody *et al.*, 2004).

In this case, the additional grouping further explains how the tree age and landscape properties contribute to AGB estimation. Both parameters are significant in determining the relationships, but they differ in the invariance of explanation. Stand age is observed as a significant factor that enhances the sensitivity of VI or biomass estimation (Zheng *et al.*, 2004; Zheng *et al.*, 2006).

According to the result, there was a significant positive relationship between model A2 and B2 (5–10 years old). Meanwhile, the older age group had a negative relationship. Models A3 and B3 (15–20 years old) exhibited a decreasing trendline, indicating reduced AGB drops as the tree age gets older. According to a previous study, the first 20 years are crucial for observing biomass formation and regeneration (Brown and Lugo, 1990). Therefore, accurate estimation of biomass and carbon storage during this period was of utmost importance. Remote sensing through the stand parameters and the VIs has proved to be a valuable tool in supporting these efforts.

The advanced discussion elaborates on the impact of VIs, which plays a crucial role in the relationship with AGB. Two indices, NDVI and further development of GNDVI, have been widely used to test and estimate AGB across regions and species. Several studies conducted on tropical and subtropical forests, as well as different kinds of plant vegetation, have produced a range of results (Sader *et al.*, 1989; Epiphanio and Huete, 1995; Gamon *et al.*, 1995; Roujean and Breon, 1995; Gitelson, Kaufman and Merzlyak, 1996; Zheng *et al.*, 2006). These studies have demonstrated that non-linear regressions generate three primary models, accommodating GNDVI, SAVI, and OSAVI as significant predictors.

A significant association with AGB in the younger age group (5–10 years old) was demonstrated by GNDVI, whereby a positive relationship was exhibited. The appearance of GNDVI in this group was attributed to the narrower canopy cover, which allowed the red and green reflectance to operate appropriately with minimal interference from the soil background. According to Sader *et al.* (1989), explained that NDVI served as a good predictor for young-age plantation forests, particularly when terrain conditions were relatively stable. In the other groups, SAVI was observed due to variations in age and landscape conditions. When tree age gets older, canopy cover becomes denser yet multilayered, leading to increased soil noise and the potential saturation of NDVI or GNDVI in capturing spectral reflectance. Therefore, employing soil line indices like SAVI or OSAVI is more suitable for elucidating the expected relationship. In Epiphanio and Huete (1995) stated that NDVI varied primarily with red reflectance, while SAVI was more responsive to NIR reflectance. The NDVI tends to saturate over densely vegetated areas, losing sensitivity to high variation in green biomass (Gitelson, Kaufman and Merzlyak, 1996). Moreover, Huete *et al.* (1997), in their comparative study of VIs, reported that SAVI is highly responsive to vegetation canopy due to its increased sensitivity to NIR spectral variations and its resistance to saturation in densely vegetated forests. Conversely, OSAVI possesses vital characteristics such as less absorbing, enhanced penetration, and scattering properties of the NIR, enabling increased sensitivity to green biomass and preventing VI saturation in areas with high vegetation cover.

Table 4. Non-linear regression model per equation and categories ($p > |t|$ varies between 0.000 to 0.1)

Model	Grouping	Number of samples	Equation	Model	R^2	Standard error		RMSE
						α	β	
A1	all age groups	66	$Y = \alpha(X/(X + \beta))$	$AGB = 13.10946*(SAVI/(SAVI-0.3693378))$	0.66	7.848	0.108	28.537
A2	age 5–10 years old	30	$Y = \alpha \exp(X\beta)$	$AGB = 3.91 * E^{-11 * \exp(GNDVI * 32.3816)}$	0.66	3.74E–10	32.381	26.907
A3	age 15–20 years old	36	$Y = \alpha(X/(X + \beta))$	$AGB = 4.957304*(OSAVI/(OSAVI-0.7822596))$	0.73	2.962	0.058	26.335
A4	valley	30	$Y = \alpha(X/(X + \beta))$	$AGB = 10.38183*(SAVI/(SAVI-0.4300787))$	0.67	6.168	0.070	32.735
A5	hill	36	$Y = \alpha(X/(X + \beta))$	$AGB = 11.31257*(SAVI/(SAVI-0.3695781))$	0.69	8.811	0.136	23.892
B1	all age groups	66	$Y = \alpha(X/(X + \beta))$	$AGB = 15.38765*(SAVI/(SAVI-0.3903365))$	0.61	8.982	0.092	41.881
B2	age 5–10 years old	30	$Y = \alpha \exp(X\beta)$	$AGB = 7.09E-20 * \exp(GNDVI * 56.13145)$	0.69	1.01E–18	16.511	37.610
B3	age 15–20 years old	36	$Y = \alpha(X/(X + \beta))$	$AGB = 6.3947*(OSAVI/(OSAVI-0.7863006))$	0.71	3.832	0.056	37.037
B4	valley	30	$Y = \alpha(X/(X + \beta))$	$AGB = 15.09414*(SAVI/(SAVI-0.4218439))$	0.61	10.892	0.092	50.491
B5	hill	36	$Y = \alpha(X/(X + \beta))$	$AGB = 10.36624*(SAVI/(SAVI-0.4203744))$	0.67	5.950	0.068	31.814

Explanations: α = model coefficient, β = model coefficient, SAVI, GNDVI, OSAVI as in Tab. 2.
Source: own study.

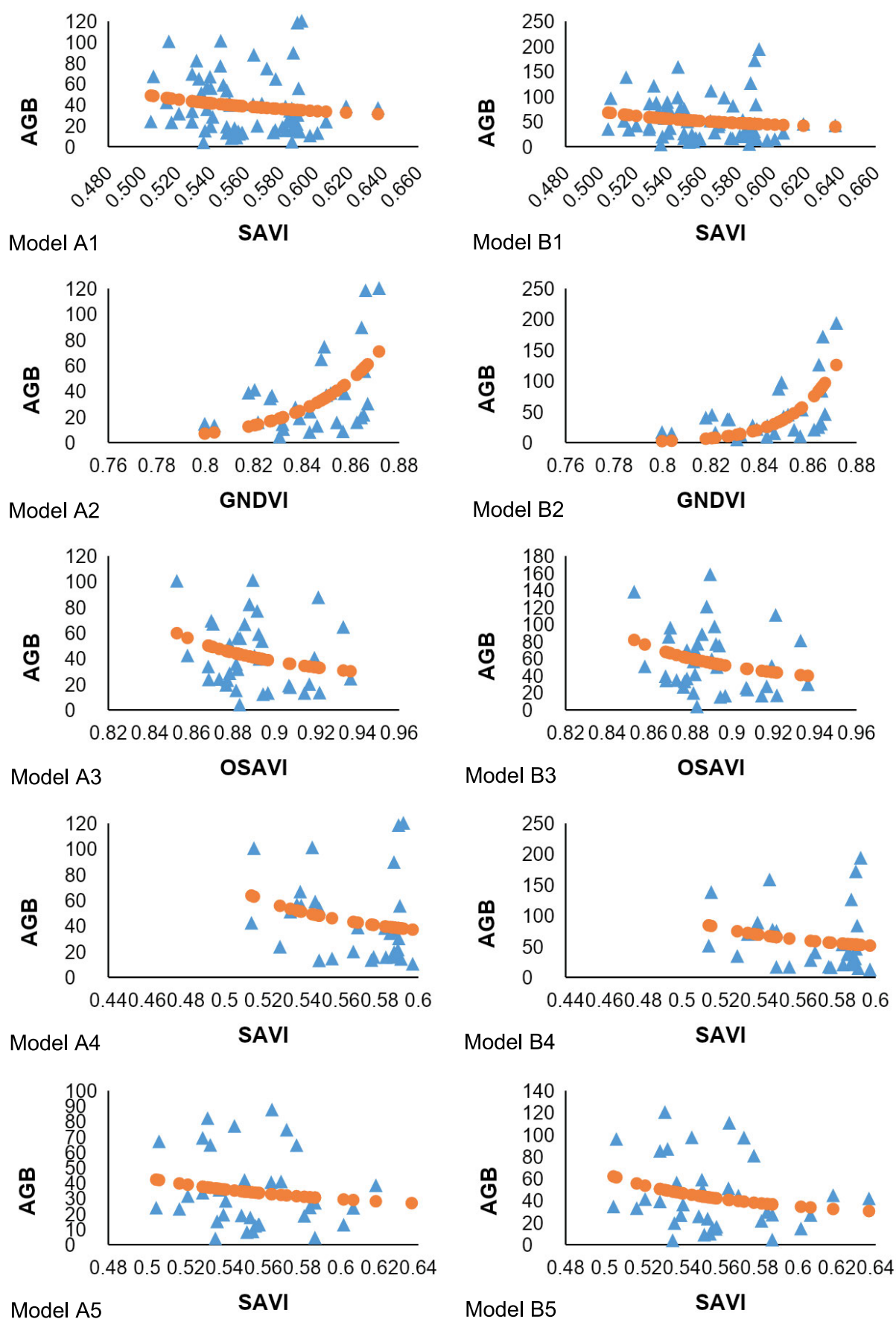


Fig. 2. Relationship between VIs and AGB (Mg·ha⁻¹) of rubber according to each model ($p > |t|$ varies between 0.000 and 0.1); SAVI, GNDVI, OSAVI as in Tab. 2, models as in Tab. 4; source: own study

POSSIBILITY OF ERROR

The previous models and results are still prone to errors that can be improved in future studies. Similarly, an analysis of errors using *RSME* was conducted for specific groupings. It was found that *RMSE* for the predictions varied along with the grouping, as shown in Table 5. When comparing the predicted *AGB* of both models, model A1 had less *RMSE* than model B1 (“all age groups” category with 66 samples). The value of model A1 is 28.537 Mg·ha⁻¹, representing a 46.8% reduction in comparison to B1, which stood at 41.881 Mg·ha⁻¹.

Table 5. Root mean square error (*RMSE*) of estimated above-ground biomass (*AGB*)

Grouping	n samples	Model	<i>RMSE</i>	
			model A	model B
All age groups	66	1	28.537	41.881
Age 5–10 years old	30	2	27.258	37.196
Age 15–20 years old	36	3	26.335	37.037
Valley	30	4	32.735	50.491
Hill	36	5	23.892	31.814

Source: own study.

A significant gap in *RMSE* was also discovered consistently across other groups (age and valley-hilly groups). In the age group models (5–10-years-old and 15–20-years-old groups), the gap between models A and B exceeded 36% (36.5% between A2 and B2, 40.6% between A3 and B3). Similarly, in the landscape group, the gap between models A and B was over 33% (33.2% between A5 and B5, 54.2% between A4 and B4). According to this trend, model A had the preferred estimated *AGB* since it has lower *RSME* value. From this result, it can also be inferred that

the main model might overestimate or underestimate by 28.537 Mg·ha⁻¹ and 41.881 Mg·ha⁻¹, for A1 and B1, respectively. Therefore, this information should be considered when using these models to generate the *predicted* biomass map.

RESULTS OF ESTIMATED ABOVEGROUND BIOMASS

The difference between the mean value of observed and estimated *AGB* is less than 1%, specifically in categories 1 (all age group), 3 (15–20 years old), and 4 (valley). However, in model A2, the difference amounted to 3.29% and increased to 9.27% in B2. The highest mean value difference between observed and estimated *AGB* was discovered in category 5 (hill), exceeding 20% (Tab. 6). Furthermore, when examining the maximum and minimum values, the discrepancy becomes more pronounced. The average gap between the maximum and minimum was significantly higher in the observed *AGB*. In both models (A and B), the average gap of the observed *AGB* at 106.561 and 166.381, respectively, was over 65% higher than the estimated value of 30.644 and 51.634.

The difference described can be attributed to the inherent variance in the estimation results, given that all the estimated values are generated from mathematical models. In an effort to enhance compatibility, several adjustments were implemented, such as selecting a single input as the predictor and discarding other possible variables that could influence the predicted *AGB* value. However, the framework of this model was reasonably suitable for elucidating the relationship between *VI*s and *AGB*, which constitutes one of the primary objectives of this study.

Upon examining the prediction line, it becomes evident that it follows a decreasing trend, consistent with the negative relationship between *VI*s and *AGB*, as shown in Figure 3. The inclusion of *VI*s has an impact on reducing the estimated *AGB* values. This result has been elaborated on in the previous section, highlighting that the saturation point was likely the primary explanation for this negative direction. As biomass reaches its

Table 6. The statistic of estimated aboveground biomass (*AGB*) for model A and model B

Grouping	Number of sample	Model	Observed AGB			Estimated AGB			A difference of mean value (%)
			mean	min.	max.	mean	min.	max.	
Model A									
All age groups	66	A1	38.981	3.722	123.348	38.963	31.227	48.877	0.05
Age 5–10 years old	30	A2	35.201	4.235	123.348	34.044	6.911	70.939	3.29
Age 15–20 years old	36	A3	42.131	3.722	100.833	41.967	30.084	59.786	0.39
Valley	30	A4	44.663	10.105	123.348	44.578	37.119	63.675	0.19
Hill	36	A5	34.247	3.722	87.432	43.919	26.971	42.253	22.02
Model B									
All age groups	66	B1	51.662	3.462	193.372	51.628	39.780	67.905	0.07
Age 5–10 years old	30	B2	45.773	4.062	193.372	41.529	2.224	125.942	9.27
Age 15–20 years old	36	B3	56.569	3.462	157.957	56.375	39.850	81.795	0.34
Valley	30	B4	60.952	11.914	193.372	60.848	51.431	84.293	0.17
Hill	36	B5	34.235	3.462	120.195	43.908	30.522	62.040	22.03

Explanations: models as in Tab. 4.

Source: own study.

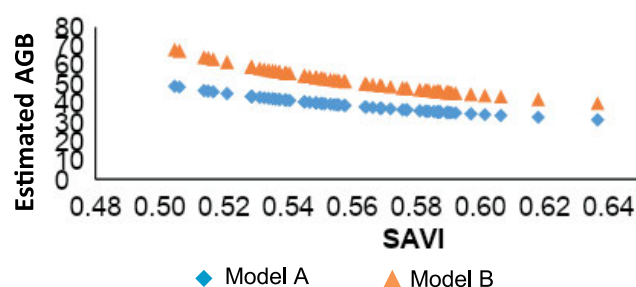


Fig. 3. Estimated aboveground biomass (AGB, Mg-ha⁻¹) per equation; source: own study

peak at around 8 years, its level subsequently decreases and saturates as the trees mature (Sone *et al.*, 2014). The difference is noticeable when analysing different age groups, particularly the 5–10-years (models A2 and B2), where the predicted AGB line increases along with the addition of the VI value. In contrast, the 15–20-year-old group (models A3 and B3) exhibits a decreasing trend. Since the total number of tree samples for the 15–20-year group exceeds its 5–10-years counterpart, the results of the entire model development tend to have a negative relationship toward AGB value.

SPATIAL DISTRIBUTION OF PREDICTED ABOVEGROUND BIOMASS

In the following analysis, the model developments were executed against the VIs throughout the entire area of Felda Lubuk Merbau. This was conducted using a mapping program intended to attain the spatial distribution of modelled AGB. The total area encompasses 2,906.41 ha and is classified into two different classes, namely rubber and non-rubber. The non-rubber region consists of bare land (land preparation) and the built-up area. Meanwhile, the rubber region was classified into three groups, namely all-age-group, 5–10-years-old, and 15–20-year-old. The models are constructed through the model function of estimated AGB derived from non-linear tests. Consequently, their naming remains the same.

The variable of landscape area (hill and valley) has not been included in the classification process as it is not directly related to the variance of VIs value analysed in this study. It had a robust relationship in determining AGB, but cannot be clearly interpreted and distinguished. Further investigation using more suitable satellite sensors that are specifically designed to

differentiate landscape variables should be considered for a more comprehensive analysis. Consequently, the spatial distribution of modelled AGB was presented solely based on the age group classes. In this subchapter, the AGB value is discussed as predicted, resulting from prediction models developed through the statistical tests and applied to the entire study area.

The rubber area spans 1,780.74 ha in all age groups, resulting in a total AGB of over 3 and 4 Tg for models A1 and B1, respectively, as shown in Table 7. The area distribution differed significantly in the other two classes, with the 5–10-years-old and 15–20-year-old groups covering 841.75 and 901.55 ha (about 6.6% larger than the younger group). This discrepancy had notable impacts on the total predicted AGB per class, leading to a steep value that should be anticipated. In model A, the older age group (A3) had a total AGB of 1,672,198.67 Mg. This was 37.9% higher than the total biomass of 1,037,453.79 Mg in the younger age group. Meanwhile, in model B, the older (B3) and younger age groups had a total of 2,246,326.96 and 1,109,320.57 Mg of AGB.

The results presented were obtained by determining the significant values of VIs through the earlier conducted statistical tests. The total predicted AGB values were calculated using specific functions with different VI as the variable input. The total estimation for predicted AGB in the all age group (models A1 and B1) was obtained using SAVI, where the 5–10-years-old (models A2 and B2) and 15–20 years-old groups (models A3 and B3) utilise GNDVI and OSAVI. These distinctive VIs shaped the total predicted value, which is independently estimated. They were not calculated as the summary of the two groups. Therefore, this accounted for the extensively different total AGB of the older and younger age groups. It should be noted that there were a considerable number of young trees at the age of 5 in the younger age group, having less amount of AGB than trees between the age of 15 and 20. This condition covers the dynamics of opposites relationships between the younger and older age group. Despite that this biomass peaked at age 8, the total amount remains excessively higher in the older age group.

The spatial distribution for predicted AGB for each group is observed through the distribution map shown in Figure 4. The maps show the classification of different predicted AGB values from low to high within the spatial aspects. Furthermore, the rubber plantations are divided into two sub-areas, located on the northern and southern sides. The centre area is classified as non-rubber, primarily consisting of bare land (land preparation) and

Table 7. Summary of the spatial distribution of predicted aboveground biomass (AGB) throughout the entire area of Felda Lubuk Merbau

Area ¹⁾	Extent (ha)	Statistic AGB (Mg)									
		model A					model B				
		model function	min.	max.	mean	total	model function	min.	max.	mean	total
Rubber in all age group	1,780.74	A1	28.35	50.16	38.73	3,061,630.64	B1	35.64	70.15	51.35	4,058,817.51
Rubber in 5–10 years old	841.75	A2	5.04	92.70	27.90	1,037,453.79	B2	1.29	200.34	30.04	1,109,320.57
Rubber in 15–20 years old	901.55	A3	29.54	62.19	41.80	1,672,198.67	B3	39.11	85.30	56.15	2,246,326.96

¹⁾ Non-rubber area was of 1,125.67 ha, total area was of 2,906.41 ha. Source: own study.

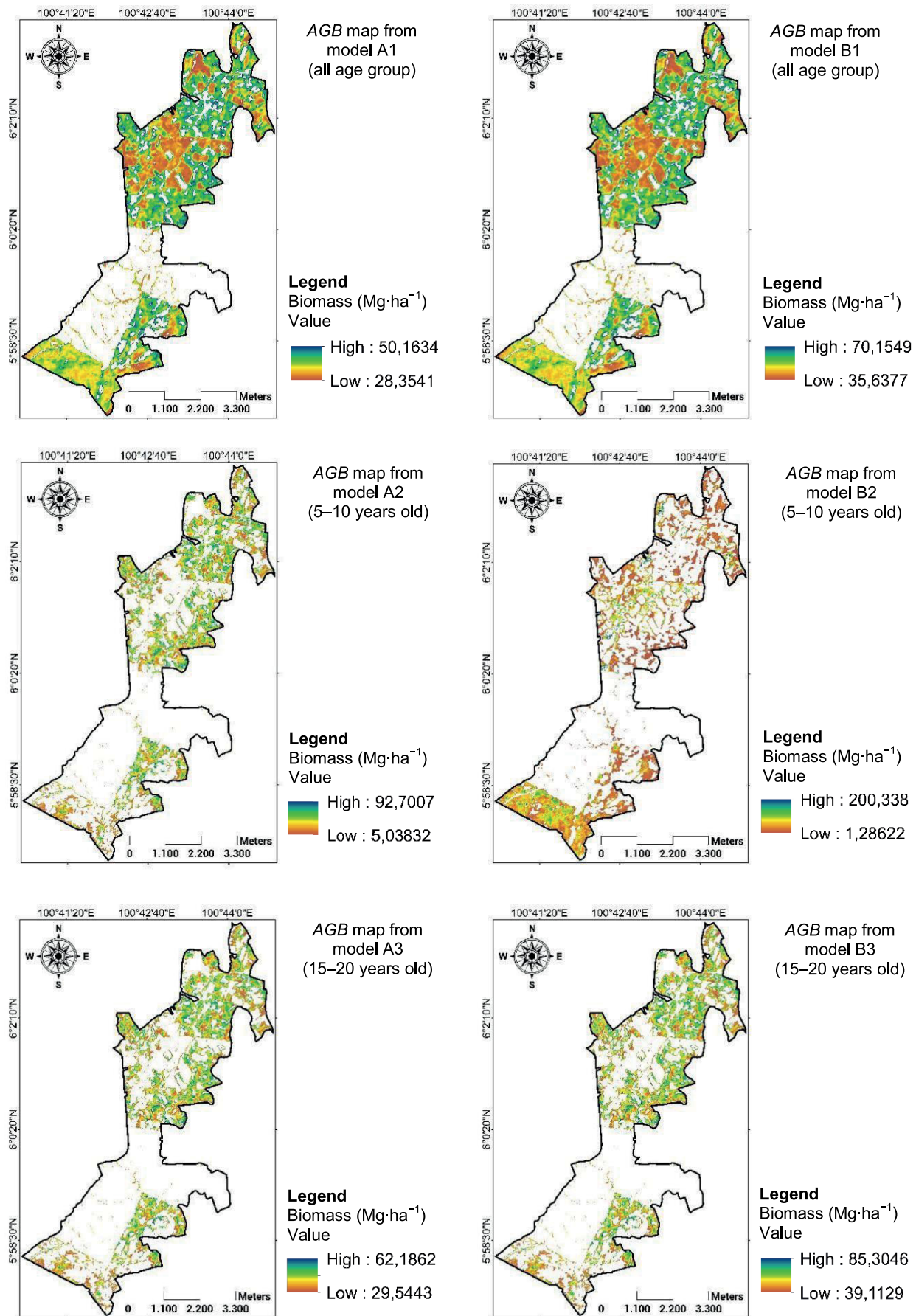


Fig. 4. Spatial distribution maps of predicted aboveground biomass (AGB) in Felda Lubuk Merbau; source: own study

built-up areas. This status of land preparation is determined by the specific time of the satellite imagery acquired in 2015. It can be observed that the amount of modelled AGB within the central area is slightly lower than in its fringe counterpart, which is indicated by the brown colour. When compared to the northern and southern sides, it is evident that the darker colour (from green to blue) indicates the area with the least amount of AGB value.

In the spatial distribution map of the “all age group” category, it is observed that some areas are without colour. It should be noted that the absence of colour does not necessarily indicate a non-rubber plantation. These areas, located between the canopy, are classified as no-colour due to the lack of spectral reflectance of VIs. This can suggest that these areas either have no canopy cover or exhibit a direct soil background, resulting in a zero AGB classification. Another possibility is that these areas possess VIs values that fall below or exceed the threshold suitable for AGB model development. As a result, they are assigned a zero value and classified as no-colour on the map.

Furthermore, the distribution maps of each age group are defined with slightly different colour-covered areas. It is observed that the 15–20-year-old group (models A3 and B3) encompasses a larger area compared to its 5–10-years-old counterpart (models A2 and B2). This corresponds to the data in Table 7, which indicated a higher predicted AGB value in the older age group. This dynamic is applied similarly in both models, as they are developed with similar input functions but with slightly different coefficient values.

CONCLUSIONS

This study successfully demonstrated that Landsat 8 OLI-TIRS data provides a highly effective and scalable remote sensing tool for accurately estimating Aboveground Biomass (AGB) in diverse rubber plantation settings. The statistical evidence strongly validates the use of non-linear regression models – specifically those utilising VIs – over simpler linear approaches for AGB estimation. The research confirms that the choice of the VI is crucial, identifying canopy- and soil-adjusted VIs (such as SAVI and OSAVI) as robust predictors, which are vital for mitigating saturation and noise effects often observed in high-biomass, heterogeneous canopies.

A key finding of this research is the significant influence of stand age and landscape heterogeneity on model performance and biomass accumulation dynamics. The study emphasises that AGB estimation models must be stratified (grouped) by age and topographic condition, as a one-size-fits-all approach is insufficient for maximising accuracy. Specifically, we observed that the rate of biomass increment is age-dependent, peaking during the young-to-mature phase and subsequently decreasing due to saturation. Furthermore, terrain correction was identified as a critical pre-processing step, particularly in areas with varying topography (hilly and valley regions), confirming the need for robust data preparation to minimise noise from shadow effects.

The overall results underscore the significance of rubber plantations in the regional carbon sequestration dynamic and provide a direct methodological contribution. The stratified mathematical models developed in this study offer forest managers and environmental agencies a reliable, cost-effective

tool to monitor biomass inventory and inform sustainable land management practices across broad spatial scales. This capacity for regional, spatially explicit carbon reporting is essential for meeting climate change mitigation goals.

While the study successfully provides an optimised approach, future research should focus on utilising more updated, higher spatial resolution satellite imagery (e.g., Sentinel-2 or commercial data) to further enhance the quality of spatial information. Additionally, incorporating a larger, more comprehensive sample size of ground-truth data will contribute to developing even more generalisable and highly accurate biomass estimation models, thereby advancing the field of carbon accounting in managed forest systems.

ACKNOWLEDGMENTS

We would like to thank Felda Lubuk Merbau staff, Mr. Yakoob, and Mr. Taufik for their assistance during the fieldwork. The authors would like to thank the Faculty of Forestry and Environment, Universiti Putra Malaysia, for the helpful laboratory assistance. The authors also would like to thank the Department of Geography, Faculty of Mathematics and Natural Sciences, for the support during the research.

FUNDING

This research is supported by Fundamental Research Grant Scheme (FRGS) from Ministry of Science, Technology and Innovation Malaysia based on contract no FRGS/1/2016/5524906.

CONFLICT OF INTERESTS

All authors declare that they have no conflicts of interest.

REFERENCES

- Anderson, G.L. and Hanson, J.D. (1992) “Evaluating hand-held radiometer derived vegetation indices for estimating above-ground biomass on semiarid rangelands,” *Geocarto International*, 7(1), pp. 71–78. Available at: [https://doi.org/10.1016/0034-4257\(93\)90040-5](https://doi.org/10.1016/0034-4257(93)90040-5).
- Anderson, G.L., Hanson, J.D. and Haas, R.H. (1993) “Evaluating Landsat Thematic Mapper derived vegetation indices for estimating above-ground biomass on semiarid rangelands,” *Remote Sensing of Environment*, 45(2), pp. 165–175. Available at: [https://doi.org/10.1016/0034-4257\(93\)90040-5](https://doi.org/10.1016/0034-4257(93)90040-5).
- Anurogo, W., Lubis, M.Z. and Mufida, M.A.K. (2018) “Modified soil-adjusted vegetation index in multispectral remote sensing data for estimating tree canopy cover density at a rubber plantation,” *Journal of Geoscience, Engineering, Environment, and Technology*, 3(1), pp. 15–24. Available at: <https://doi.org/10.24273/jgeet.2018.3.01.1003>.
- Bagheri, N. *et al.* (2012) “Soil-line vegetation indices for corn nitrogen content prediction,” *International Agrophysics*, 26(2), 103. Available at: <https://doi.org/10.2478/v10247-012-0016-8>.
- Boegh, E., Soegaard, H. and Thomsen, A. (2002) “Evaluating evapotranspiration rates and surface conditions using Landsat

- TM to estimate atmospheric resistance and surface resistance,” *Remote Sensing of Environment*, 79(2–3), pp. 329–343. Available at: [https://doi.org/10.1016/S0034-4257\(01\)00283-8](https://doi.org/10.1016/S0034-4257(01)00283-8).
- Brown, S. and Lugo, A.E. (1990) “Tropical secondary forests,” *Journal of Tropical Ecology*, 6(1), pp. 1–32. Available at: <https://doi.org/10.1017/S0266467400003989>.
- Chapman, E.C. (1991) “The expansion of rubber in southern Yunnan, China,” *Geographical Journal*, 157(1), pp. 36–44. Available at: <https://doi.org/10.2307/635142>.
- Chen, J.M. (1996) “Evaluation of vegetation indices and a modified simple ratio for boreal applications,” *Canadian Journal of Remote Sensing*, 22(3), pp. 229–242. Available at: <https://doi.org/10.1080/07038992.1996.10855178>.
- Dey, S.K. *et al.* (1996) “Estimation of biomass in *Hevea* clones by regression method: 2. Relation of girth and biomass for mature trees of clone RRIM 600,” *Journal of Natural Rubber Research*, 9(1), pp. 40–43.
- Dong, T. *et al.* (2016) “Estimating winter wheat biomass by assimilating leaf area index derived from fusion of Landsat-8 and MODIS data,” *International Journal of Applied Earth Observation and Geoinformation*, 49, pp. 63–74. Available at: <https://doi.org/10.1016/j.jag.2016.02.001>.
- Eastwood, J.A. *et al.* (1997) “The reliability of vegetation indices for monitoring saltmarsh vegetation cover,” *International Journal of Remote Sensing*, 18(18), pp. 3901–3907. Available at: <https://doi.org/10.1080/014311697216739>.
- Elvidge, C.D. and Chen, Z. (1995) “Comparison of broad-band and narrow-band red and near-infrared vegetation indices,” *Remote Sensing of Environment*, 54(1), pp. 38–48. Available at: [https://doi.org/10.1016/0034-4257\(95\)00132-K](https://doi.org/10.1016/0034-4257(95)00132-K).
- Epiphanio, J.N. and Huete, A.R. (1995) “Dependence of NDVI and SAVI on sun/sensor geometry and its effect on fAPAR relationships in alfalfa,” *Remote Sensing of Environment*, 51(3), pp. 351–360. Available at: [https://doi.org/10.1016/0034-4257\(94\)00110-9](https://doi.org/10.1016/0034-4257(94)00110-9).
- Fan, H. *et al.* (2015) “Phenology-based vegetation index differencing for mapping of rubber plantations using Landsat OLI data,” *Remote Sensing*, 7(5), pp. 6041–6058. Available at: <https://doi.org/10.3390/rs70506041>.
- Fang, J.Y. *et al.* (1998) “Forest biomass of China: An estimate based on the biomass-volume relationship,” *Ecological Applications*, 8(4), pp. 1084–1091. Available at: [https://doi.org/10.1890/1051-0761\(1998\)008\[1084:FBOCAE\]2.0.CO;2](https://doi.org/10.1890/1051-0761(1998)008[1084:FBOCAE]2.0.CO;2).
- Foody, G.M., Boyd, D.S. and Cutler, M.E. (2003) “Predictive relations of tropical forest biomass from Landsat TM data and their transferability between regions,” *Remote Sensing of Environment*, 85(4), pp. 463–474. Available at: [https://doi.org/10.1016/S0034-4257\(03\)00039-7](https://doi.org/10.1016/S0034-4257(03)00039-7).
- Foody, G.M. *et al.* (2004) “Thematic labelling from hyperspectral remotely sensed imagery: trade-offs in image properties,” *International Journal of Remote Sensing*, 25(12), pp. 2337–2363. Available at: <https://doi.org/10.1080/01431160310001654969>.
- Gamon, J.A. *et al.* (1995) “Relationships between NDVI, canopy structure, and photosynthesis in three Californian vegetation types,” *Ecological Applications*, 5(1), pp. 28–41. Available at: <https://doi.org/10.2307/1942049>.
- Gitelson, A.A., Kaufman, Y.J. and Merzlyak, M.N. (1996) “Use of a green channel in remote sensing of global vegetation from EOS-MODIS,” *Remote Sensing of Environment*, 58(3), pp. 289–298. Available at: [https://doi.org/10.1016/S0034-4257\(96\)00072-7](https://doi.org/10.1016/S0034-4257(96)00072-7).
- Goh, J. *et al.* (2013) “Biomass estimation in humid tropical forest using a combination of ALOS PALSAR and SPOT 5 satellite imagery,” *Asian Journal of Geoinformatics*, 13(4), pp. 1–10.
- Goh, K.J., Lee, C.T. and Kok, C.H. (2013) “Carbon sequestration in rubber plantations – A review,” *Journal of Rubber Research*, 16(3), pp. 163–176.
- Guo, Y. and Zeng, F. (2012) “Atmospheric correction comparison of SPOT-5 image based on model FLAASH and model QUAC,” *International Archives of the Photogrammetry, Remote Sensing and Spatial Information Sciences*, 39(7), pp. 21–23. Available at: <https://doi.org/10.5194/isprsarchives-XXXIX-B7-7-2012>.
- Haripriya, G.S. (2000) “Integrating forest resources into the system of national accounts in Maharashtra, India,” *Environment and Development Economics*, 5(1), pp. 143–156. Available at: <https://doi.org/10.1017/S1355770X00000103>.
- Heriansyah, I. *et al.* (2025) “Allometric equations model for estimating an above and below ground biomass of dipterocarp forest in the tropics,” *Global Journal of Environmental Science & Management (GJESM)*, 11(3). Available at: <https://doi.org/10.22034/gjesm.2025.03.18>.
- Houghton *et al.* (eds.) (1995) *Climate change 1995 – The science of climate change. Contribution of Working Group I to the Second Assessment Report of the Intergovernmental Panel on Climate Change*. Geneva: IPCC. Available at: https://www.ipcc.ch/site/assets/uploads/2018/02/ipcc_sar_wg_I_full_report.pdf (Accessed: January, 14, 2025).
- Huete, A.R. (1988) “A soil-adjusted vegetation index (SAVI),” *Remote Sensing of Environment*, 25(3), pp. 295–309. Available at: [https://doi.org/10.1016/0034-4257\(88\)90106-X](https://doi.org/10.1016/0034-4257(88)90106-X).
- Huete, A.R. *et al.* (1997) “A comparison of vegetation indices over a global set of TM images for EOS-MODIS,” *Remote Sensing of Environment*, 59(3), pp. 440–451. Available at: [https://doi.org/10.1016/S0034-4257\(96\)00112-5](https://doi.org/10.1016/S0034-4257(96)00112-5).
- Huete, A. *et al.* (2002) “Overview of the radiometric and biophysical performance of the MODIS vegetation indices,” *Remote Sensing of Environment*, 83(1–2), pp. 195–213. Available at: [https://doi.org/10.1016/S0034-4257\(02\)00096-2](https://doi.org/10.1016/S0034-4257(02)00096-2).
- Hui, X. (1999) “A biomass model compatible with volume,” *Journal of Beijing Forestry University*, 21(5), pp. 32–36. [In Chinese].
- Jat, M.L. *et al.* (2022) “Carbon sequestration potential, challenges, and strategies towards climate action in smallholder agricultural systems of South Asia,” *Crop and Environment*, 1(1), pp. 86–101. Available at: <https://doi.org/10.1016/j.crope.2022.03.005>.
- Laben, C.A. and Brower, B.V. (2000) *Process for enhancing the spatial resolution of multispectral imagery using pan-sharpening*. U.S. Patent No. 6,011,875. U.S. Int. Cl. G06K 9/36, U.S. Cl. 382/276; 382/254; 382/278; 382/299. Appl. No.: 09/069,232. Date of filing Apr. 29, 1998. Date of publ. Jan. 4, 2000. Available at: <https://patentimages.storage.googleapis.com/f9/72/45/c9f1fffe687d30/US6011875.pdf> (Accessed: January 14, 2025).
- Li, Z. and Fox, J.M. (2012) “Mapping rubber tree growth in mainland Southeast Asia using time-series MODIS 250 m NDVI and statistical data,” *Applied Geography*, 198(1–3), pp. 149–167. Available at: <https://doi.org/10.1016/j.apgeog.2011.06.018>.
- Lu, D. (2005) “Aboveground biomass estimation using Landsat TM data in the Brazilian Amazon,” *International Journal of Remote Sensing*, 26(12), pp. 2509–2525. Available at: <https://doi.org/10.1080/01431160500142145>.
- Lu, D. *et al.* (2004) “Relationships between forest stand parameters and Landsat TM spectral responses in the Brazilian Amazon Basin,” *Forest Ecology and Management*, 198(1–3), pp. 149–167. Available at: <https://doi.org/10.1016/j.foreco.2004.03.048>.
- Mutanga, O. and Skidmore, A.K. (2004) “Narrow band vegetation indices overcome the saturation problem in biomass estimation,” *International Journal of Remote Sensing*, 25(19), pp. 3999–4014. Available at: <https://doi.org/10.1080/01431160310001654923>.

- Nelson, B.W. *et al.* (2001) "Modeling biomass of forests in the southwest Amazon by polar ordination of Landsat TM," in *X Simpósio Brasileiro de Sensoriamento Remoto – SBSR*, Foz de Iguaçu, Paraná, Brazil, 21–26 Apr 2001. São José dos Campos: INPE, pp. 1683–1690.
- Nelson, R., Short, A. and Valenti, M. (2004) "Measuring biomass and carbon in Delaware using an airborne profiling LIDAR," *Scandinavian Journal of Forest Research*, 19(6), pp. 500–511. Available at: <https://doi.org/10.1080/02827580410019508>.
- Phua, M.H. and Saito, H. (2003) "Estimation of biomass of a mountainous tropical forest using Landsat TM data," *Canadian Journal of Remote Sensing*, 29(4), pp. 429–440. Available at: <https://doi.org/10.5589/m03-005>.
- Popescu, S.C., Wynne, R.H. and Nelson, R.F. (2003) "Measuring individual tree crown diameter with lidar and assessing its influence on estimating forest volume and biomass," *Canadian Journal of Remote Sensing*, 29(5), pp. 564–577. Available at: <https://doi.org/10.5589/m03-027>.
- Qi, J. *et al.* (1994) "A modified soil adjusted vegetation index," *Remote Sensing of Environment*, 48(2), pp. 119–126. Available at: [https://doi.org/10.1016/0034-4257\(94\)90134-1](https://doi.org/10.1016/0034-4257(94)90134-1).
- Rondeaux, G., Steven, M. and Baret, F. (1996). "Optimization of soil-adjusted vegetation indices," *Remote Sensing of Environment*, 55(2), pp. 95–107. Available at: [https://doi.org/10.1016/0034-4257\(95\)00186-7](https://doi.org/10.1016/0034-4257(95)00186-7).
- Roujean, J.L. and Breon, F.M. (1995) "Estimating PAR absorbed by vegetation from bidirectional reflectance measurements," *Remote Sensing of Environment*, 51(3), pp. 375–384. Available at: [https://doi.org/10.1016/0034-4257\(94\)00114-3](https://doi.org/10.1016/0034-4257(94)00114-3).
- Rouse Jr., J.W. *et al.* (1974) *Monitoring the vernal advancement and retrogradation (green wave effect) of natural vegetation*. Texas: Remote Sensing Center Texas A&M University, College Station. Available at: <https://ntrs.nasa.gov/api/citations/19750020419/downloads/19750020419.pdf> (Accessed: January 14, 2025).
- Roy, P.S. and Ravan, S.A. (1996) "Biomass estimation using satellite remote sensing data-an investigation on possible approaches for natural forest," *Journal of Biosciences*, 21(4), pp. 535–561. Available at: <https://doi.org/10.1007/BF02703218>.
- Sader, S.A. *et al.* (1989) "Tropical forest biomass and successional age class relationships to a vegetation index derived from Landsat TM data," *Remote Sensing of Environment*, 28, pp. 143–198. Available at: [https://doi.org/10.1016/0034-4257\(89\)90112-0](https://doi.org/10.1016/0034-4257(89)90112-0).
- Sarker, L.R. and Nichol, J.E. (2011) "Improved forest biomass estimates using ALOS AVNIR-2 texture indices," *Remote Sensing of Environment*, 115(4), pp. 968–977. Available at: [https://doi.org/10.1016/0034-4257\(89\)90112-0](https://doi.org/10.1016/0034-4257(89)90112-0).
- Sekrecka, A., Kedzierski, M. and Wierzbicki, D. (2019) "Pre-processing of panchromatic images to improve object detection in pansharpened images," *Sensors*, 19(23), 5146. Available at: <https://doi.org/10.3390/s19235146>.
- Shidiq, I.P.A. and Ismail, M.H. (2016) "Stand age model for mapping spatial distribution of rubber tree using remotely sensed data in Kedah, Malaysia," *Jurnal Teknologi*, 78(5), pp. 239–244. Available at: <https://doi.org/10.11113/jt.v78.8303>.
- Shorrocks, V.M., Templeton, J.K. and Iyer, G.C. (1965) "Mineral nutrition, growth and nutrient cycle of *Hevea brasiliensis*: 3. Relationship between girth and shoot dry weight," *Journal of Rubber Research Institute of Malaya*, 19, pp. 85–92.
- Sone, K. *et al.* (2014) "Carbon sequestration, tree biomass growth and rubber yield of PB260 clone of rubber tree (*Hevea brasiliensis*) in North Sumatra," *Journal of Rubber Research*, 17(2), pp. 115–127.
- Steininger, M.K. (2000) "Satellite estimation of tropical secondary forest above-ground biomass: Data from Brazil and Bolivia," *International Journal of Remote Sensing*, 21(6–7), pp. 1139–1157. Available at: <https://doi.org/10.1080/014311600210119>.
- Thenkabail, P.S. *et al.* (2004) "Biomass estimations and carbon stock calculations in the oil palm plantations of African derived savannas using IKONOS data," *International Journal of Remote Sensing*, 25(23), pp. 5447–5472. Available at: <https://doi.org/10.1080/01431160412331291279>.
- USGS (2019) *Landsat 8 (L8) data users handbook. LDS-1574 Version 5.0*. Sioux Falls: Department of the Interior US Geological Survey. Available at: https://d9-wret.s3.us-west-2.amazonaws.com/assets/palladium/production/s3fs-public/atoms/files/LSDS-1574_L8_Data_Users_Handbook-v5.0.pdf (Accessed: January 14, 2025).
- Wang, J. *et al.* (2019) "Estimating leaf area index and aboveground biomass of grazing pastures using Sentinel-1, Sentinel-2 and Landsat images," *Journal of Photogrammetry and Remote Sensing*, 154, pp. 189–201. Available at: <https://doi.org/10.1016/j.isprsjprs.2019.06.007>.
- Wu, Y. and Starhler, A. (1994) "Remote estimation of crown size, stand density, and biomass on the Oregon transect," *Ecological Applications*, 4(2), pp. 299–312. Available at: <https://doi.org/10.2307/1941935>.
- Yan, F., Wu, B. and Wang, Y. (2013) "Estimating aboveground biomass in Mu Us Sandy Land using Landsat spectral derived vegetation indices over the past 30 years," *Journal of Arid Land*, 5(4), pp. 521–530. Available at: <https://doi.org/10.1007/s40333-013-0180-0>.
- Yuan, J. and Niu, Z. (2008) "Evaluation of atmospheric correction using FLAASH," 2008 *International Workshop on Earth Observation and Remote Sensing Applications*, pp. 1–6. Available at: <https://doi.org/10.1109/EORSA.2008.4620341>.
- Zhang, G. *et al.* (2014) "Estimation of forest aboveground biomass in California using canopy height and leaf area index estimated from satellite data," *Remote Sensing of Environment*, 151, pp. 44–56. Available at: <https://doi.org/10.1016/j.rse.2014.01.025>.
- Zheng, D. *et al.* (2004) "Estimating aboveground biomass using Landsat 7 ETM+ data across a managed landscape in northern Wisconsin, USA," *Remote Sensing of Environment*, 93(3), pp. 402–411. Available at: <https://doi.org/10.1016/j.rse.2004.08.008>.
- Zheng, G. *et al.* (2007) "Combining remote sensing imagery and forest age inventory for biomass mapping," *Journal of Environmental Management*, 85(3), pp. 616–623. Available at: <https://doi.org/10.1016/j.jenvman.2006.07.015>.
- Zheng, Z. *et al.* (2006) "Forest structure and biomass of a tropical seasonal rain forest in Xishuangbanna, Southwest China," *Biotropica: The Journal of Biology and Conservation*, 38(3), pp. 318–327. Available at: <https://doi.org/10.1111/j.1744-7429.2006.00148.x>.
- Zhu, X. and Liu, D. (2015) "Improving forest aboveground biomass estimation using seasonal Landsat NDVI time-series," *ISPRS Journal of Photogrammetry and Remote Sensing*, 102, pp. 222–231. Available at: <https://doi.org/10.1016/j.isprsjprs.2014.08.014>.
- Ziegler, A.D., Fox, J.M. and Xu, J. (2009) "The rubber juggernaut. The demise of swidden cultivation in Southeast Asia may have devastating environmental consequences," *Science*, 324(5930), pp. 1024–1025. Available at: <https://doi.org/10.1126/science.1173833>.